

Numerical validations of the method of assessing the nature of grounding-line steady states

Supplementary document for
“Suppression of marine ice sheet instability”

by Sam Pegler

This supplementary document presents a suite of bifurcation diagrams and accompanying numerical solutions in order to illustrate the method of assessing the natures of stability of the steady state proposed in §2.2 of the paper. The method is based on evaluating the function $V(x)$ defined by (3.3), and using its sign to infer the nature of local stability. If the gradient of V at the steady state is negative, then it is an attractor. If instead it is positive, then it is a repeller.

Each example involves the illustrative bedrock profile,

$$b(x) = -\beta_m + \alpha(x - x_m) \tanh[k(x - x_m)]. \quad (1)$$

representing a localised topographic maximum or minimum, depending on whether $\alpha < 0$ or $\alpha > 0$. The topographic maximum is set as $x_m = -10^3$, and the sharpness parameter $k = 10^{-3}$. For each example, I vary the slope scale α and reference ocean depth β_m , assume linear rheology, $n = 1$, and a calving position at $x_C = 0$.

In examples (a) to (c), distributed accumulation is neglected downstream of the ice divide, with a localised input of dimensionless flux equal to unity. In example (d), a large-scale non-zero distribution is assumed with no-flux at the ice divide.

Example 1

For this example, I set $\alpha = 10^{-3}$, $\beta_m = 3.2$, and $x_D = -2 \times 10^3$, with a localised input flux equal to unity at the ice divide. The bifurcation diagram showing the variation of steady states against the dimensionless shear drag parameter S is shown in figure (a). Red represents regions where $V < 0$, light green represents regions where $V > 0$ and dark green represents regions where secondary grounding affects the steady state. For values of $S < 5.0 \times 10^{-4}$, there is a pair of steady states: an attractor along the positively sloped region downstream ($x \lesssim 400$), and a repeller in the upstream region ($x \gtrsim 400$). For $S > 5.0 \times 10^{-4}$, there are no steady states and the grounding-line advances unconditionally to long times.

The two steady states for $S = 4.5 \times 10^{-4}$ are shown in figures (b, c). Four time-dependent numerical solutions determined using my Lagrangian solver of the full unsimplified initial-value problem are shown in figure (d). The solutions were each initiated with grounding-line positions slightly upstream and downstream of the steady states. The numerical solutions confirm the natures of local stability for each steady state inferred from the direction of sign switches in V .

Example 2

For this example, I set the same specifications as example 1, except with the slightly shallower ocean depth $\beta_m = 2.8$, and $x_D = -2 \times 10^3$. Interestingly, the bifurcation diagram shown in figure (a) is qualitatively different. There is a single, stable steady state occurring for all $S > 9 \times 10^{-5}$. The steady state for $S = 10^{-4}$ is shown in figure b. The inferred nature of stability is indicated in figure (c) by two numerical solutions of the full unsimplified model.

Example 3

For this example, I set $\alpha = -10^{-3}$, $\beta_m = 3.2$, and $x_D = -2 \times 10^3$, producing a profile with a topographic maximum in the bed profile. The stability portrait of figure 3(a) indicates two steady states for $S > 4.4 \times 10^{-4}$ and unconditional retreat otherwise. The downstream steady state, arising for $x \gtrsim -1500$, is an attractor, while the upstream steady state, arising for $x \lesssim -1500$, is a repeller. The stable steady state for $S = 5 \times 10^{-4}$ is shown in figure 3(b) and the nature of its stability verified in figure 4(b).

Example 4

For this example, I set $\alpha = -10^{-3}$, $\beta_m = 3$ and $x_D = -10^3$. In contrast to the cases above, I assume the distributed accumulation

$$F(x) = F_0 \left[1 - \left(\frac{x - x_D}{x_D} \right)^2 \right], \quad (2)$$

where $F_0 = 2 \times 10^{-3}$ is a dimensionless reference rate of accumulation, which is illustrated in figure 4(b). The stability portrait of figure 4(a) shows a single repelling steady state for $S < 6.7 \times 10^{-4}$ and unconditional advance for $S > 6.7 \times 10^{-4}$. The steady state for $S = 5 \times 10^{-4}$ is shown in figure 4(b). The inferred nature of its stability is confirmed by the time-dependent numerical solutions of the full simplified model shown in figure 4(c).

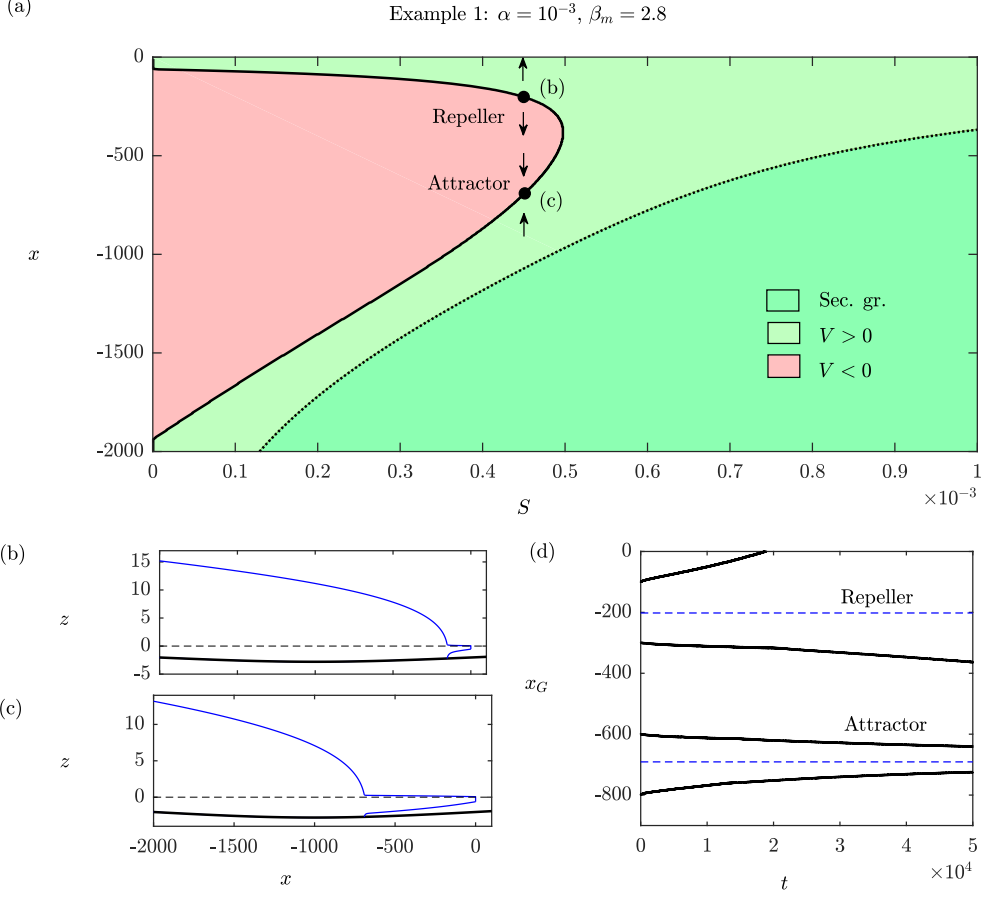


Figure 1: Example 1, given by $\alpha = 10^{-3}$, $\beta_m = 3.2$, and $x_D = -2 \times 10^3$. Panel (a) shows the bifurcation diagram with colour indicating the sign of the stability variable V . Panel (b) shows the profiles of the two steady states occurring for $S = 4.5 \times 10^{-4}$. Panel (c) shows the grounding line evolution predicted by numerical solutions of the full model, confirming the stability properties inferred from the bifurcation diagram: the downstream state is a repeller while the upstream state is an attractor.

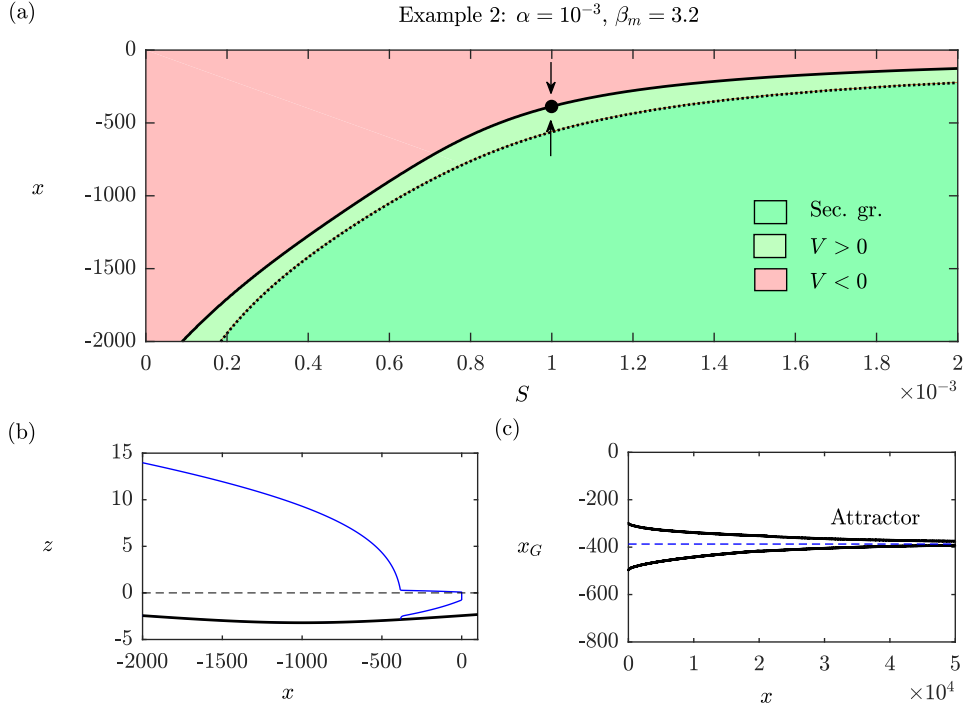


Figure 2: Example 2, given by $\alpha = 10^{-3}$, $\beta_m = 2.8$ and $x_D = -2 \times 10^3$. Panel (a) shows the bifurcation diagram with colour indicating the sign of the stability variable V . Panel (b) shows the profile of the steady state occurring for $S = 10^{-3}$. Panel (c) shows the grounding-line evolution predicted by numerical solutions of the full model, confirming that the steady state is a repeller

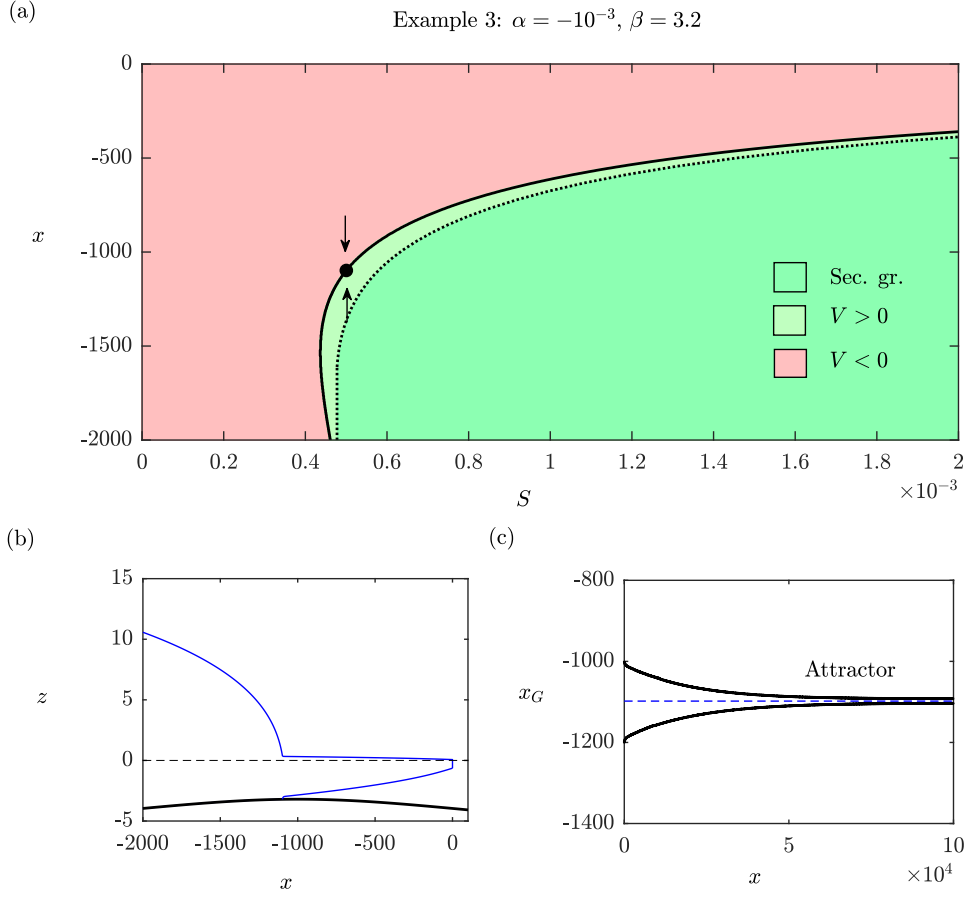


Figure 3: Example 3, given by $\alpha = -10^{-3}$, $\beta_m = 3.2$ and $x_D = -2 \times 10^3$. Panel (a) shows the bifurcation diagram with colour indicating the sign of the stability variable V . Panel (b) shows the profile of the steady state occurring for $S = 5 \times 10^{-4}$. Panel (c) shows the grounding-line evolution predicted by numerical solutions of the full model, confirming that the steady state is an attractor.

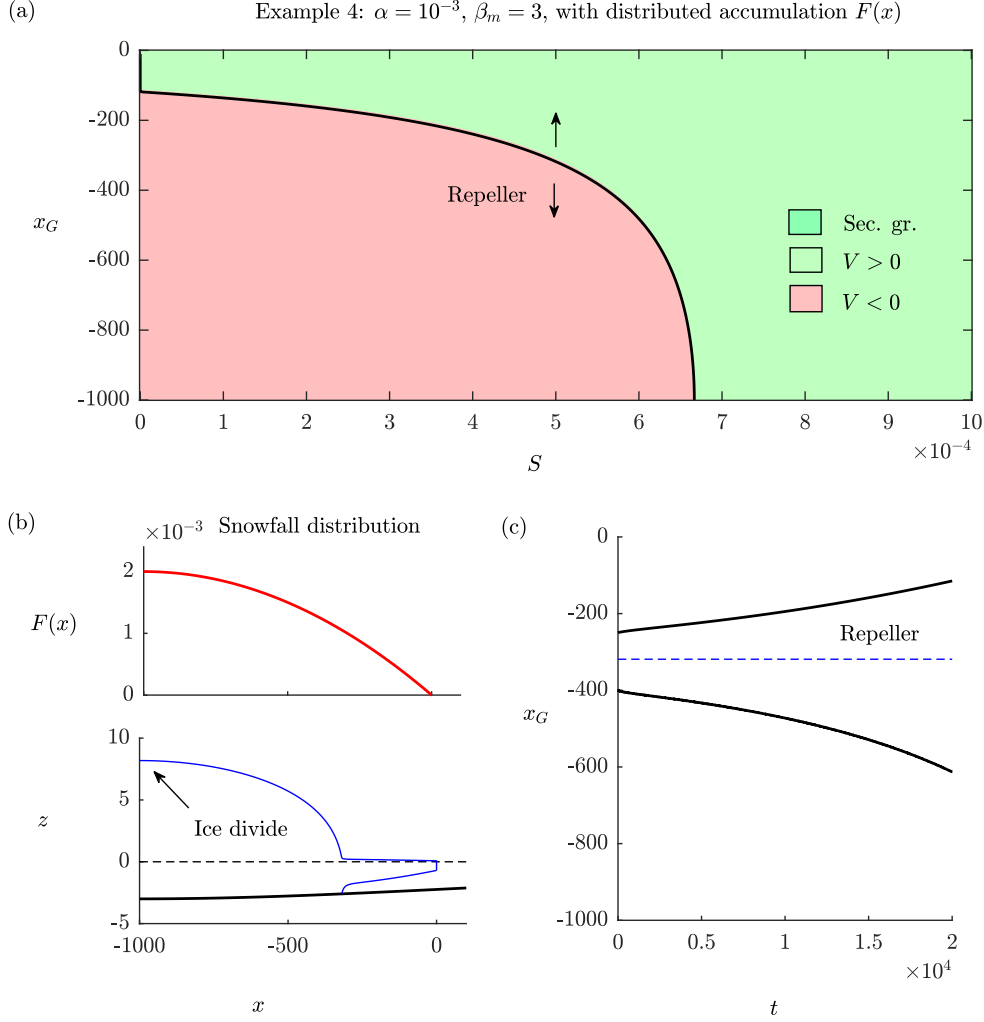


Figure 4: Example 4, given by $\alpha = -10^{-3}$, $\beta_m = 3$ and $x_D = -10^3$. This example involves a distributed accumulation field specified by (2), which is illustrated in panel (b). Panel (a) shows the bifurcation diagram with colour indicating the sign of the stability variable V . Panel (b) shows the accumulation field (upper plot) and the profile of the steady state occurring for $S = 5 \times 10^{-4}$ (lower plot). Panel (c) shows the grounding-line evolution predicted by numerical solutions of the full model, confirming that the steady state is a repeller.